Progress In Electromagnetics Research, PIER 103, 67–100, 2010

FIELD AND SOURCE EQUIVALENCE IN SOURCE RECONSTRUCTION ON 3D SURFACES

J. L. Araque Quijano and G. Vecchi

Antenna and EMC Lab
Politecnico di Torino
Corso Duca degli Abruzzi 24, 10129, Turin, Italy

Abstract—This paper describes in detail different formulations of the inverse-source problem, whereby equivalent sources and/or fields are to be computed on an arbitrary 3-D closed surface from the knowledge of complex vector electric field data at a specified (exterior) surface. The starting point is the analysis of the formulation in terms of the Equivalence Principle, of the possible choices for the internal fields, and of their practical impact. Love's (zero interior field) equivalence is the only equivalence form that yields currents directly related to the fields on the reconstruction surface; its enforcement results in a pair of coupled integral equations. Formulations resulting in a single integral equation are also analyzed. The first is the single-equation, two-current formulation which is most common in current literature, in which no interior field condition is enforced. The single-current (electric or magnetic) formulation deriving from continuity enforcement of one field is also introduced and analyzed. Single-equation formulations result in a simpler implementation and a lower computational load than the dual-equation formulation, but numerical tests with synthetic data support the benefits of the latter. The spectrum of the involved (discretized) operators clearly shows a relation with the theoretical Degrees of Freedom (DoF) of the measured field for the dual-equation formulation that guarantees extraction of these DoF; this is absent in the single-equation formulation. Examples confirm that single-equation formulations do not yield Love's currents, as observed both with comparison with reference data and via energetic considerations. The presentation is concluded with a test on measured data which shows the stability and usefulness of the dual-equation formulation in a situation of practical relevance.

Corresponding author: G. Vecchi (giuseppe.vecchi@polito.it).

1. INTRODUCTION

Source reconstruction techniques have various applications in antenna engineering: antenna diagnostics from field measurements, compact antenna representation, and near field to far field (NF-FF) transformation. The source reconstruction problem is a linear inverse problem where the aim is obtaining currents with known location that radiate a given complex vector field (usually resulting from measurements), and/or information on the fields via the computed currents. The problem is naturally formulated in terms of integral equations, and has been addressed by several works, some of which are rather recent, showing an ongoing interest in the subject. Proceeding in chronological order, [36] presented the application of equivalent magnetic currents on an infinitely extended plane in near-to-far field transformation, discussing the possibility of obtaining a globally valid pattern representation; [8, 37] present a similar application, and the method is compared to wave expansion techniques; [38] addressed global field extrapolation from its knowledge on a limited region using equivalent magnetic currents lying on an infinite Perfect Electric Conductor (PEC) plane, and [39] did the dual (electric currents/Perfect Magnetic Conductor (PMC)). In [34], the computation of far field from near-field measurements on a limited range is demonstrated. In [24], the use of equivalent magnetic currents is reported for small antennas diagnostics; [35] presents a (2-D) scalar treatment of the source reconstruction problem for axisymmetric structures with explicit enforcement of the so-called extinction theorem. In [23], the source reconstruction technique is used to characterize commercial antennas from measurements over a limited canonical range using a model based on equivalent magnetic currents on planar surfaces; [22] presents the use of source reconstruction for antenna diagnostics obtaining indications of primary radiators on a 3-D surface enclosing the actual radiator; [3] discusses the use of the Rao-Wilton-Glisson (RWG) basis for current expansion and an Singular Value Decomposition (SVD)-based regularization technique, while [1] presents an approach to source reconstruction based on the integral equation for arbitrary 3-D geometries and the use of electric and magnetic currents; [25] uses Hertzian electric dipoles as equivalent sources for the determination of complex array excitations from near field measurements. The work in [26] compares planar magnetic source reconstruction to spherical-wave-to-plane-wave transformation in diagnostic tasks showing comparable performances. In [4], a novel diagnostic application is presented of the source reconstruction technique, whereby disturbances present in measurements due to

unwanted interaction with neighboring objects are removed in a post-processing step; finally, [5] introduced the dual-equation formulation for the general vector problem on 3-D surfaces and showed its advantages over the widespread single-equation formulation.

A different, more theoretically-oriented line of research exists, e.g., [28–30], but apparently these works have not been considered in most of the previously cited literature (some of these results will be employed here).

On the algorithmic side, it can be noted that fast factorizations methods for integral equations have a very natural application in source reconstruction and have been exploited recently: [2] presents the acceleration of planar magnetic source reconstruction via the Fast Multipole Method (FMM), while [14] presents the Multi-Level Fast Multipole Method (ML-FMM) implementation of the conventional formulation [1] of source reconstruction using the Rao-Wilton-Glisson (RWG) basis and both electric and magnetic currents.

The main objective of this work is a unified framework of the various possible formulations of the source reconstruction problem, and the discussion of their most relevant features, applications and limitations — as supported by analytical considerations and numerical results. To the best of our knowledge such a treatment has not been published elsewhere; yet, we will show that it is necessary for understanding and proper utilization of the technique.

With the exception of [5, 35], the works found in literature deal with the source reconstruction problem in terms of a single integral equation even when both electric and magnetic equivalent currents are being sought for; uniqueness issues are not addressed: we will show here that they impact on the quality of the results, and — perhaps more importantly — on their meaning and interpretation in diagnostics applications.

It is important to observe that the desired output of a source reconstruction may be of two, rather different types. In some cases, the reconstructed sources are not important per se, being only required to well reproduce the given (e.g., measured) field upon radiation; this is the case for NF-FF applications. Other times, one would like to know the *fields* on a specified reconstruction surface, and typically so in diagnostics applications; in this case, we will show that this directly impacts on the formulation, requiring to formulate the problem in terms of two coupled integral equations.

The source reconstruction problem is considered an ill-posed one, and therefore its singular-value spectrum plays an important role in assessing the stability to real-life noisy and otherwise non-ideal data, and the related ability to obtain a given spatial resolution. We will

address also this issue.

The various formulations of the problem are tested on synthetic field data that allow assessing the accuracy of field reconstruction inwards of the measurement surface; the results show that only Dual-Equation Formulation (DEqF) is guaranteed to provide equivalent currents directly related to electric and magnetic fields on general 3-D reconstruction surfaces. Finally, tests on measured data confirm the higher accuracy and stability of the Dual-Equation Formulation.

2. FORMULATION

The input data for the problem are the values of the electric field tangent to a specified measurement surface denoted by Σ_M, or the outcome of a linear operator applied to it; the latter instance accounts for the interference of the measuring system with the field. Σ_M is typically a sphere or a cylinder, and may be open (like a finite cylinder, or a finite planar domain).

The aim is finding sources on a closed "reconstruction surface", denoted by Σ_R, that radiate the input field on Σ_M; in certain instances, one may also be interested in the actual field values on Σ_R. The reconstruction surface Σ_R encloses a volume Ω_-, $\Sigma_R = \partial\Omega_-$ which contains all material that differs from free space, and the original sources of the problem. The region Ω_- need not be connected (i.e., it may also consist of a set of disjoint regions, so that Σ_R becomes a set of closed surfaces). We stress that the two objectives of finding equivalent sources or tangent fields on Σ_R may be identical, but only if this is required and enforced, as discussed in the next sections.

The measured (or anyway given) field is known in amplitude and phase; since the reconstruction surface is assigned, the source reconstruction problem is linear. It will be formulated in terms of integral equations upon application of the Equivalence Principle[†] for the general (and practically relevant) case of a fully 3-D reconstruction surface Σ_R. The integral equations are subsequently discretized and solved by the Method of Moments.

2.1. Equivalent Sources and Fields

The first step is the application of the Equivalence Principle [6, 20]. Consider the original radiation problem, depicted in Fig. 1(left); the volume Ω_- contains all the original sources, and all material bodies (like antenna conductors, other obstacles, etc.), while the

[†] Because of its nature, we prefer the term Equivalence *Theorem*, but we conform here to the more common terminology.

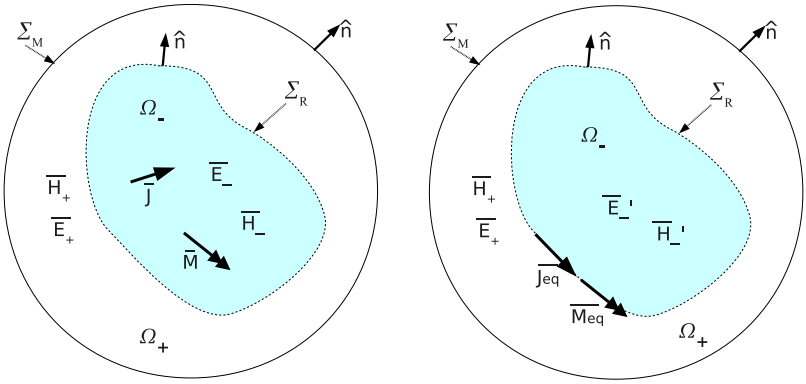

Figure 1. Illustration of the Equivalence Principle: Original (left) and general equivalent problem (right).

external region is in free space. In the external equivalent problem in Fig. 1(right), original sources and material bodies have been removed and equivalent electric and magnetic currents, $\mathbf{J}_{eq}$ and $\mathbf{M}_{eq}$ are placed on the enclosing surface such that external fields $\mathbf{E}_+$, $\mathbf{H}_+$ remain unchanged, while the original inner fields $\mathbf{E}_-$, $\mathbf{H}_-$ are substituted by other fields, denoted by $\mathbf{E}_-{}', \mathbf{H}_-{}'$. In order to achieve this, i.e., field equivalence in Ω_+, these equivalent currents must obey:

$$\left.\begin{array}{c} \hat{\mathbf{n}} \times [\mathbf{H}_+(\mathbf{r}) - \mathbf{H}_-{}'(\mathbf{r})] = \mathbf{J}_{eq} \\ -\hat{\mathbf{n}} \times [\mathbf{E}_+(\mathbf{r}) - \mathbf{E}_-{}'(\mathbf{r})] = \mathbf{M}_{eq} \end{array}\right\} \mathbf{r} \in \Sigma_R \tag{1}$$

Irrespective of the choice of the internal fields $\mathbf{E}_-{}', \mathbf{H}_-{}'$, due to the removal of all internal material bodies, the equivalent currents $\mathbf{J}_{eq}$, $\mathbf{M}_{eq}$ radiate in unbounded homogeneous space and thus, fields due to these can be computed everywhere by using the conventional free-space radiation operator:

$$\mathbf{E}(\mathbf{r}) = -\eta_0 \mathcal{L}(\mathbf{J}_{eq}; \mathbf{r}) + \mathcal{K}(\mathbf{M}_{eq}; \mathbf{r}) \tag{2}$$

where

$$\begin{aligned} \mathcal{L}(\mathbf{J}_{eq}; \mathbf{r}) &= jk_0 \int_{\Sigma_R} \left[\mathbf{J}_{eq}(\mathbf{r}') + \frac{1}{k_0^2} \nabla \nabla_s' \cdot \mathbf{J}_{eq}(\mathbf{r}') \right] g(\mathbf{r}, \mathbf{r}') ds' \\ \mathcal{K}(\mathbf{M}_{eq}; \mathbf{r}) &= \int_{\Sigma_R} \mathbf{M}_{eq}(\mathbf{r}') \times \nabla g(\mathbf{r}, \mathbf{r}') ds' \\ g(\mathbf{r}, \mathbf{r}') &= \frac{e^{-jk_0|\mathbf{r}-\mathbf{r}'|}}{4\pi|\mathbf{r}-\mathbf{r}'|} \end{aligned} \tag{3}$$

where $\eta_0 = \sqrt{\mu_0/\epsilon_0}$, $k_0 = \omega\sqrt{\mu_0\epsilon_0}$, and ∇_s' is the surface divergence operator ($\mathbf{r} \notin \Sigma_R$).

Indeed, as discussed in [6, P. 654] (we have translated the original terms to make the statement clear under our notation; brackets [] indicate those translated versions):

"The current densities of [(1)] are said to be equivalent only within $[\Omega_+]$, because they produce the original fields $[\mathbf{E}_+, \mathbf{H}_+]$ only outside $[\Sigma_R]$. Fields $[\mathbf{E}'_-, \mathbf{H}'_-]$ different from the originals $[\mathbf{E}_-, \mathbf{H}_-]$, result within Ω_-. Since the currents of [(1)] radiate in an unbounded space, the fields can be determined using [(2)] ..."

When using equivalence as stated above, the internal fields $\mathbf{E}_-, \mathbf{H}_-$ constitute a degree of freedom, but of course not just any internal field can be used for this purpose: internal fields determine equivalent currents, but the internal fields must be effectively radiated by these as given by (2), otherwise the jump conditions in (1) are simply violated. This shows that the internal field must be one that can be radiated by sources outside Ω_-, or equivalently, a field that satisfies homogeneous Maxwell's equations in Ω_-, i.e., no sources therein.

While infinitely many currents and internal fields are possible (see e.g., [20, P. 107]), because of the above-mentioned self-consistency requirement only some of the choices are practically useful in setting up *direct problems*, as recalled below. In this sense, before proceeding it is important to stress that the use of field equivalence in this inverse problem is — or may be — rather different from its application in direct problems. In particular, in direct problems the boundary of $\Sigma_R = \partial\Omega_-$ will represent a material discontinuity boundary, where one must enforce boundary conditions. On the other hand, all the present problem requires, as stated at the start of this section, is to radiate fields from the reconstruction surface Σ_R up to the measurement surface Σ_M, where we enforce the field to a boundary value; we are not interested in the field radiated *inside* the reconstruction surface because *in general* we do not have to enforce boundary conditions on Σ_R; this is, e.g., the conventional approach followed in [1].

Instead, the choice of the modified internal fields $(\mathbf{E}_-{}', \mathbf{H}_-{}')$ determines the physical meaning of the equivalent currents, i.e., the relationship between these currents and the actual fields at the reconstruction surface Σ_R.

In the following, we analyze those choices for the internal fields that lead to a well-defined meaning of the equivalent currents; this also corresponds to those choices that are viable for the setup of integral equations for the direct problem.

2.1.1. Zero Interior Field

If one sets the interior fields equal to zero, the result is Love's form of the Equivalence Principle:

$$\left.\begin{array}{c}\hat{\mathbf{n}}\times\mathbf{H}_{+}(\mathbf{r})=\mathbf{J}_{eq}^{Love}\\ -\hat{\mathbf{n}}\times\mathbf{E}_{+}(\mathbf{r})=\mathbf{M}_{eq}^{Love}\end{array}\right\}\mathbf{r}\in\Sigma_{n} \tag{4}$$

With Love's equivalence, fields on the boundary are obtained directly from the equivalent currents, which is very important in antenna diagnostic applications.

Filling the interior with a PEC or PMC can suppress one of the two equivalent currents and yet let them remain consistent with the actual fields on the surface Σ_R via (4); however, to do so one must obviously use of the Green's function for the considered surface and the specified impedance boundary condition on such a surface. When an infinite plane can be of interest as the support for the sought-for equivalent currents, (e.g., as in [23, 24, 34, 36, 38, 39]) this is obviously easy.

2.1.2. Single-current Formulation

The possibility of employing a single equivalent current *without* requiring the Green's function of a body occupying Σ_R has received attention in direct methods because of the obvious economy in the number of unknowns. From (1), it can be seen that an equivalent problem involving only electric (or magnetic) currents in a homogeneous medium is obtained by requiring the interior $E(H)$ fields to have tangential components equal to the actual fields [17, 31, 32]. In [31], the problem is solved explicitly for the case of a spherical surface. As apparent from (1) and recalled in the cited literature, the equivalent current in this case is *not* related to the field as simply as in Love's form of equivalence; i.e., if one uses the electric current, this is not simply $\hat{\mathbf{n}}\times\mathbf{H}$ on the reconstruction surface. With the exception of the very recent [33] for the special case of a spherical surface, we are not aware of published work on this formulation in connection with inverse-source problems; however, we will show that it it carries significant illustrative value, and perspectives of practical applicability.

2.2. Integral Equation Setup and Uniqueness

According to the discussion above, irrespective of the choice of the internal fields, fields radiated by the currents on Σ_R in the region *external* to Σ_R — and in particular on the measurement surface Σ_M — are obtained by using the Green's function of the free space (see

Fig. 1(right)). The component of E tangential to Σ_M is linked to equivalent sources as follows

$$\hat{\mathbf{n}} \times \mathbf{E}(\mathbf{r}) = \hat{\mathbf{n}} \times [-\eta_0 \mathcal{L}(\mathbf{J}_{eq}; \mathbf{r}) + \mathcal{K}(\mathbf{M}_{eq}; \mathbf{r})] \quad \mathbf{r} \in \Sigma_M \tag{5}$$

where operators were defined in (3).

Enforcing the radiated field to be equal to the measured field, one sets up an integral equation for the two unknown currents on Σ_R.

Note that unless one enforces some other condition explicitly, currents obtained by solving (5) in general will radiate a non-zero field in Ω_-, which is not in disagreement with theory, just the manifestation of an unspecified boundary condition on $\Sigma_R = \partial\Omega_-$. Also, we repeat that the equivalent currents are not unique, and so is the solution to (5). This is hopefully clarified by the examples in the following discussion. One may consider setting $\mathbf{M}_{eq}$ to zero; as discussed in Section 2.1, this corresponds to the choice of the equivalence in which the tangential E field is continuous across Σ_R; likewise by setting $\mathbf{J}_{eq} = 0$. Considering also the case in which no additional condition is imposed, we have three different current sets that radiate the same field at Σ_M and thus rigorously solve (5); furthermore, at least two of these (J-only, M-only) are guaranteed to radiate non-zero fields inside Σ_R due to the continuity imposed by the absence of one of the currents. Indeed, field equivalence prescribes only that fields radiated by the equivalent currents be identical outside Σ_R; these differ inside as the result of the arbitrary choice of the interior field.

The non-uniqueness of solution to (5) can be seen also from the perspectives of the properties of the integral equation itself. When equivalent currents are reconstructed resorting to (5) alone, it has been shown in the literature (e.g., see [28]) that there is a null space associated with the radiation operator involved, that corresponds to the non-radiating sources, i.e., sources radiating exactly zero field — as opposed to reactive fields that are non-zero away from the actual source of radiation, but often negligible in practice.

A throughout characterization of such non-radiating sources set is beyond our scope (the interested reader can consult e.g., [28]), but it is enlightening to construct a linear sub-space thereof as follows. It is shown in the classic reference [40, Eq. (17)] that Love's equivalent sources corresponding to sources completely on one side of Σ_R (either inside or outside) are mapped through the radiation operator in (5) to a field that is discontinuous in traversing Σ_R, being identically zero in the volume where original sources were located and equal to the original one elsewhere. We note further that this result holds irrespective of whether the volume containing the actual sources is the interior or exterior one. We can therefore set up an *interior* equivalent problem corresponding to an arbitrary arrangement of sources outside Σ_R by

computing Love's equivalent currents $\mathbf{J}_{eq} = \hat{\mathbf{n}} \times \mathbf{H}$ and $\mathbf{M}_{eq} = -\hat{\mathbf{n}} \times \mathbf{E}$ on Σ_R that radiate the same fields inside Σ_R as the original ones (note that $\hat{\mathbf{n}}$ points inside Σ_R this time). According to the cited reference, these sources radiate zero field outside Σ_R (in particular on Σ_M), and therefore belong to the aforementioned null space.

It should be noted that this lack of uniqueness is overlooked in the literature on source reconstruction; this is not surprising, though: as explained next, it does not prevent convergence of iterative solvers. In fact, the (almost always) rectangular linear system arising upon discretization of (5) is solved resorting to the method of normal equations [18], which is equivalent to using the Moore-Penrose pseudo-inverse, and thus leads to the minimum-norm solution[‡] of the associated least-squares problem [13, Eq. (5), 28]; i.e., the null-space is removed from the solution. Otherwise said, the actually solved problem corresponds to the explicit equation in (5), *plus* the minimum-norm condition on the reconstructed currents. The solution to this modified problem is unique [13, 28]: whether this is the sought-after solution or not remains to be ascertained. We will investigate on this by relating the solution of this inverse problem to the choice of the interior fields in the initial equivalence setting.

We begin by observing that there is no warranty that the minimum-norm equivalent sources obtained via (5) radiate zero internal field, and — while this cannot be excluded a priori — it appears unlikely because this would imply a large reactive component in the currents, that conflicts with the minimum norm condition. The non-zero field arising in this case will be indeed apparent from the numerical tests presented in Section 3.

If the minimum-norm solution does not radiate zero fields inside Σ_R, the associated currents are *not* Love's equivalent currents. If one wants to reconstruct Love's equivalent currents, a source distribution has to be added to the minimum-norm solution in order to cancel out fields inside Σ_R, but subject to the constraint that those outside remain unchanged. This means adding a source distribution that radiates a zero field outside Σ_R (and in particular at the measurement surface), and a (specified) non-zero field inside the reconstruction surface. This source distribution is therefore an element of the of the null (sub-)space constructed above.

Phrased now again in terms of the field equivalence principle, equivalent currents that radiate a given field in the volume outside Σ_R (and in particular on Σ_M) are not unique; fields radiated by all possible equivalent currents are identical outside Σ_R but differ inside: the normal equation solution of (5) chooses those internal fields leading

[‡] In the sense of the ℓ_2 norm, i.e., the coefficient norm

to equivalent currents with minimum norm.

From the above it can be concluded that if one wants to obtain the actual fields on the reconstruction surface directly from the currents in (5), the zero field condition of Love's equivalence has to be explicitly enforced, which is obtained by demanding that tangential fields just inside Σ_R (hence the notation Σ_R^-) are zero:

$$\hat{\mathbf{n}} \times \mathbf{E}_-(\mathbf{r}) = \lim_{\mathbf{r}\to\Sigma_R^-} \hat{\mathbf{n}} \times \left[-\eta_0 \mathcal{L}(\mathbf{J}_{eq}^{Love};\mathbf{r}) + \mathcal{K}(\mathbf{M}_{eq}^{Love};\mathbf{r})\right] = 0 \quad (6a)$$

$$\hat{\mathbf{n}} \times \mathbf{H}_-(\mathbf{r}) = \lim_{\mathbf{r}\to\Sigma_R^-} \hat{\mathbf{n}} \times \left[-\frac{1}{\eta_0}\mathcal{L}(\mathbf{M}_{eq}^{Love};\mathbf{r}) - \mathcal{K}(\mathbf{J}_{eq}^{Love};\mathbf{r})\right] = 0 \quad (6b)$$

We recall that in our equivalent problems we have no sources inside Ω_- (the fields are solution to the homogeneous Maxwell equations), so that by uniqueness [20, P. 101–102] specifying $\hat{\mathbf{n}}\times\mathbf{E} = 0$ on $\Sigma_R = \partial\Omega_-$, $\mathbf{E}$ is zero everywhere in Ω_- and hence so is $\mathbf{H}$. The converse holds for specifying $\hat{\mathbf{n}} \times \mathbf{H}$, so that it is enough to enforce any one of (6a), (6b).

The arbitrariness of the limiting enforcement surface Σ_R^- can be removed with a more general formulation [5]; it can be shown [5, 21, Eqs. (6), (29)] that the equations above are equivalent to the following boundary integral identities:

$$\hat{\mathbf{n}} \times \left[-\eta_0 \mathcal{L}(\mathbf{J}_{eq}^{Love};\mathbf{r}) + \mathcal{K}(\mathbf{M}_{eq}^{Love};\mathbf{r})\right] = -\frac{1}{2}\mathbf{M}_{eq}^{Love}(\mathbf{r}) \quad \mathbf{r} \in \Sigma_R \quad (7a)$$

$$\hat{\mathbf{n}} \times \left[-\frac{1}{\eta_0}\mathcal{L}(\mathbf{M}_{eq}^{Love};\mathbf{r}) - \mathcal{K}(\mathbf{J}_{eq}^{Love};\mathbf{r})\right] = \frac{1}{2}\mathbf{J}_{eq}^{Love}(\mathbf{r}) \quad \mathbf{r} \in \Sigma_R \quad (7b)$$

Again, the same reasoning on uniqueness applies to enforcing any one of (7a), (7b).

We observe that in the form (6) this additional constraint is similar to that used in direct problems to remove spurious resonances [41, 42], and essentially as in [35]; in its form (7) it is similar to the approach to re-condition the equation for scattering by dielectric bodies [15, 43].

It is worth mentioning that addition of Love's condition to the conventional integral Equation (5) yields a system of two equations for two unknowns, as opposed to the more common formulation in which two unknown currents are computed from a single equation. When the reconstruction surface tends to the measurement surface, $\Sigma_R \to \Sigma_M$, (5) together with (6) allows the determination of electric and magnetic currents as in (4) via specification of the (measured) E field. We further note that the case where zero-field enforcement is not effected (conventional formulation), or one of the currents is absent is derived from the former in a trivial manner. Therefore, formulations used in [1–3, 14, 22–25, 34, 36, 38, 39] are all particular cases of the general one presented here.

The on-surface conditions enforced in the integral Equation (7) or (6) imply spectral properties of the involved operators opposite to those of the measured-field enforcement (5), and this is expected to significantly alter the spectrum of the resulting linear system, with a lessening of the ill-posedness of the inverse-source problem; this will be verified in the results of Section 3.

For ease of reference in comparing the various formulations, they will be labeled as follows: Single-Equation Formulations (SEqFs) refer to the sole use of (5), and encompass Two-current Single-Equation Formulation (JM-SEqF), which includes both J and M currents, and the two one-current formulations: J-current Single-Equation Formulation (J-SEqF), where only J current is present and M-current Single-Equation Formulation (M-SEqF), that considers only M current. Finally, the term Dual-Equation Formulation (DEqF) refers to the addition of Love's condition with both J and M currents, i.e., based on the solution of the system (5), (6a) or variations thereof as discussed above. According to this scheme, every formulation considered can be trivially obtained from Dual-Equation Formulation (DEqF), the most general one.

At this point one may assert some metric properties of the solution to the source reconstruction problem that depend on the equivalence formulation employed. It has been stated that the inverse source problem in principle consists in solving (5), and that the solution to that equation is not unique, i.e., it is more precise to talk of a solution set rather than *the* solution. Adoption of a specific form of equivalence entails a constraint on the solution set above, i.e., only a subset of the original solution set remains valid. Concerning the solution sets generated by all formulations (those that obey the related integral equations), we can state the following membership relations:

$$\begin{aligned}(\mathbf{J}_{eq},\mathbf{M}_{eq})^{DEqF} &\in (\mathbf{J}_{eq},\mathbf{M}_{eq})^{JM\text{-}SEqF}\\ (\mathbf{J}_{eq},\mathbf{M}_{eq})^{J\text{-}SEqF} &\in (\mathbf{J}_{eq},\mathbf{M}_{eq})^{JM\text{-}SEqF}\\ (\mathbf{J}_{eq},\mathbf{M}_{eq})^{M\text{-}SEqF} &\in (\mathbf{J}_{eq},\mathbf{M}_{eq})^{JM\text{-}SEqF}\end{aligned} \tag{8}$$

Given that the normal equation solution of the arising linear system selects the minimum-norm element among these sets, the above membership relations can be used to obtain the following relationships between the ℓ_2 norm of the various solutions (MN refers to selection of the set element with minimum norm):

$$\begin{aligned}||(\mathbf{J}_{eq},\mathbf{M}_{eq})_{MN}^{DEqF}||_{\ell_2} &\geq ||(\mathbf{J}_{eq},\mathbf{M}_{eq})_{MN}^{JM-SEqF}||_{l_2}\\ ||(\mathbf{J}_{eq},\mathbf{M}_{eq})_{MN})^{J-SEqF}||_{\ell_2} &\geq ||(\mathbf{J}_{eq},\mathbf{M}_{eq})_{MN}^{JM-SEqF}||_{l_2}\\ ||(\mathbf{J}_{eq},\mathbf{M}_{eq})_{MN}^{M-SEqF}||_{\ell_2} &\geq ||(\mathbf{J}_{eq},\mathbf{M}_{eq})_{MN}^{JM-SEqF}||_{l_2}\end{aligned} \tag{9}$$

The above is intuitive by thinking that having a larger set to choose from can never lead to a worst choice (i.e., higher ℓ_2 norm). The interesting result is that the solution of (5) alone will in principle yield the lowest coefficient norm among all possible equivalence formulations; this will be confirmed by results on synthetic and measured data to be presented in Section 5.

We observe that all formulations (single- and dual-equation) are in principle not free of the problems due to the resonances of the cavity corresponding to the closed surface Σ_R, although based on least-squares solution of the associated problem. However, in our experience and in the cited literature this has never emerged as a practical occurrence.

Finally, we observe that — if desired — the actual fields and Love's currents could be recovered in a trivial way from the single-equation solution; to do so, it is enough to apply the radiation operators and/or field boundary integral identities (e.g., [21]). However, as we will see, the properties of the Dual-Equation formulation afford a more stable solution and a higher accuracy.

2.3. Discretization

The system (5), (6) of coupled integral equations is discretized via standard Method of Moments (MoM). Initially Σ_R is discretized by a mesh composed of triangular facets whose average edge size is denoted by h_R, and the unknown currents are approximated in terms of the RWG basis with $N_T = 2N$ elements in total:

$$\mathbf{J}_{eq} = \sum_{n=1}^{N} C_n^J \mathbf{f}_n \quad \mathbf{M}_{eq} = \eta_0 \sum_{n=1}^{N} C_n^M \mathbf{f}_n \tag{10}$$

(as usual, unknowns have been normalized to get uniform physical dimensions, and the same basis is used for $\mathbf{J}_{eq}$ and $\mathbf{M}_{eq}$).

In a second stage, (5) is tested by projection onto vector Dirac-delta functions coincident with the position and direction of the available field samples on Σ_M. The number of such measurements is denoted by N_m, and in standard measurement ranges it is twice the number of measurement points considering both tangential components, i.e., $N_m = 2M_s$.

As to the interior-field constraint, we note that (7) requires the evaluation of singular terms; the integrals required in the exact testing of the system (5), (7) are all standard terms of MoM (for dielectric bodies and/or EFIE and MFIE), but for simplicity of implementation we have pursued a different route.

While proper handling of the singularities plays an important role preserving the spectral properties of the discretized operators, it has been shown in [16] that the source and testing points may be displaced (in situations like this), provided the displacement is controlled by the mesh size. Therefore, we employed an approximate testing on a surface $\Sigma_R^{=}$ lying at a distance $\Delta \approx h_R$ underneath Σ_R. Within this approximation, (6) and (7) are equivalent. The testing of the inner field constraint is implemented by first building an inward-offset version of the triangular discretization of Σ_R (denoted by $\Sigma_R^{=}$) and then using a fairly uniform grid of vector tangential Dirac-delta functions on it as testing elements. The testing procedure thus leads to the following linear system:

$$\mathrm{Ax} = \mathrm{b} \tag{11a}$$

$$\eta_0 \begin{bmatrix} -\mathrm{L}_{MR} & \mathrm{K}_{MR} \\ -\mathrm{L}_{RR} & \mathrm{K}_{RR} \end{bmatrix} \begin{bmatrix} \mathrm{C}^{\mathrm{J}} \\ \mathrm{C}^{\mathrm{M}} \end{bmatrix} = \begin{bmatrix} \mathrm{E} \\ 0 \end{bmatrix} \tag{11b}$$

where the matrix counterparts of operators $\mathcal{L}$ and $\mathcal{K}$ have been subscripted by two letters indicating respectively the testing domain and the source domain, M for Σ_M, R for Σ_R.

Matrix components are obtained by projection on the testing basis (superscript on the testing functions $\mathbf{w}$ indicates the testing surface as above):

$$X_{\dagger R[m,n]} = \left\langle \mathbf{w}_m^{\dagger} | \mathcal{X}(\mathbf{f}_n) \right\rangle \tag{12a}$$

$$E_m = \left\langle \mathbf{w}_m^{\dagger} | \mathbf{E} \right\rangle \tag{12b}$$

$$X = L \text{ or } K \quad \mathcal{X} = \mathcal{L} \text{ or } \mathcal{K} \dagger = M \text{ or } R$$

The overall system matrix has dimension $(N_m + N_R) \times N_T$; in the following we will denote the total number of equations by $M_T = N_m + N_R$. Note that if one does not want to enforce the zero field condition (6) or (7), one simply deletes the second (block) row of (11b).

The rectangular linear system (11) is solved by applying the Conjugate Gradient (CG) iterative solver to the normal equation. Use of an iterative solver is mandatory for large-scale problems, allowing the application of fast algorithms as in [2, 14]. It has the additional advantage of being inherently regularizing, which is important in this inverse problem. Of particular appeal is the possibility of setting a goal residual in agreement with the tolerance of the acquisition system for improved robustness against noise, which unavoidably corrupts measurements.

3. NUMERICAL TESTS

In this section, we apply the various formulations of source reconstruction to data both generated synthetically and from measurements. In the tests with synthetic data, the field samples at Σ_M are computed via (MoM) simulation of the CAD model of a given structure, as well as the fields at the reconstruction surface Σ_R; this allows evaluating the accuracy with which *fields* are reconstructed thereon.

The tests with measurement data obviously allow to test the robustness of the algorithms in real-life situations. On the other hand, while the reconstructed fields on Σ_R can be assessed qualitatively (checking symmetries, relative values, etc.) this does not allow to assess the accuracy of the reconstruction; therefore, to add a quantitative assessment, we have used measured data for a structure which we could also simulate: this is discussed in Section 5.

Finally, for the smaller problem where it was feasible, we have also conducted a study of the SV spectrum, which yields key information on the ability to reconstruct sources with a given signal-to-noise ratio in the measured field.

In agreement with the most widespread measurement setups, the general formulation presented above is restricted to the particular case of uniform spherical ranges providing for each measurement point theta and phi components of the electric field. The choice of the number of measurement points is related to the number of the DoF of the field [10–12], i.e., the minimum number of measurement samples that are necessary to reconstruct the field (at the measurement surface or farther) with negligible information loss. When the field DoF can be determined, they are useful in the reconstruction process by providing a lower bound to the resolution required in measurement setups. We employ a conservative modification of the expression found in the references above which is in agreement with the "empirical expression" found in [19, Eqs. (2.1) and (4.137)]); it allows accounting for i) small radiators and ii) near field measurements, to estimate the maximum angular interval (in radians) allowed in spherical-range measurements when the radiating structure may be enclosed by a sphere with radius a:

$$\Delta\alpha = \frac{1}{2a/\lambda + 10/\pi} \tag{13}$$

In evaluating the performance of reconstruction we use two indicators: data misfit and reconstruction error. Data misfit, which is the difference between the reconstructed ($\mathbf{E}_R$) and measured ($\mathbf{E}$)

field data, is always available, and is computed as follows:

$$\varepsilon_M = \sqrt{\frac{\iint\limits_{\Sigma_M} |\mathbf{E}_R - \mathbf{E}|^2 ds}{\iint\limits_{\Sigma_M} |\mathbf{E}|^2 ds}} \tag{14}$$

The obvious parameter to judge the quality of the reconstruction is deviation from the exact value of the currents, i.e.,

$$\varepsilon_R = \frac{\mathcal{M}(\mathbf{J}_{ex} - \mathbf{J}_R, \mathbf{M}_{ex} - \mathbf{M}_R)}{\mathcal{M}(\mathbf{J}_{ex}, \mathbf{M}_{ex})} \quad \mathcal{M}(\mathbf{J}, \mathbf{M}) = \sqrt{\iint\limits_{\Sigma_R} |\mathbf{J}|^2 + |(\mathbf{M})/\eta_0|^2 ds} \tag{15}$$

where $\mathbf{J}_{ex}$, $\mathbf{M}_{ex}$ are the exact currents and $\mathbf{J}_R$, $\mathbf{M}_R$ result from the solution of the problem in (11). The function $\mathcal{M}$ has Ampere (A) units and plays the role of "total magnitude". The exact currents are not available in real life, and as discussed above we will assess the reconstruction error in test cases where we can compute a reference solution for the currents.

It should be noted that minimizing the data misfit ε_M in (14) does not in any way imply minimization of the current reconstruction error ε_R in (15); due to the ill-conditioning of the problem two very different solutions may radiate very similar fields at the measurement surface.

3.1. Dipole on Box

The first test structure is shown in Fig. 2. It is a resonant strip dipole placed above a rectangular metallic box, and fed by a coaxial cable via a twin-lead transition. It is contained in a sphere of radius 0.43λ; therefore, according to (13), the maximum angular interval for measurements is 14.2 degrees, meaning that in a spherical range at least 314 measurements are required per field component.

3.1.1. Singular Value Analysis

We begin by analyzing the Singular Value (SV) distribution for this reconstruction problem, reported in Fig. 3 for near- and far-field measurements; all choices for the formulation are shown. In the reference reconstruction problem Σ_R is the minimum sphere (0.43λ radius) discretized by $N = 774$ RWG basis functions ($h_R = 0.1\lambda$ was used), yielding $N_T = 774$ for one-current formulations (J-current Single-Equation Formulation (J-SEqF). M-current Single-Equation Formulation (M-SEqF)) and twice as many for two-current

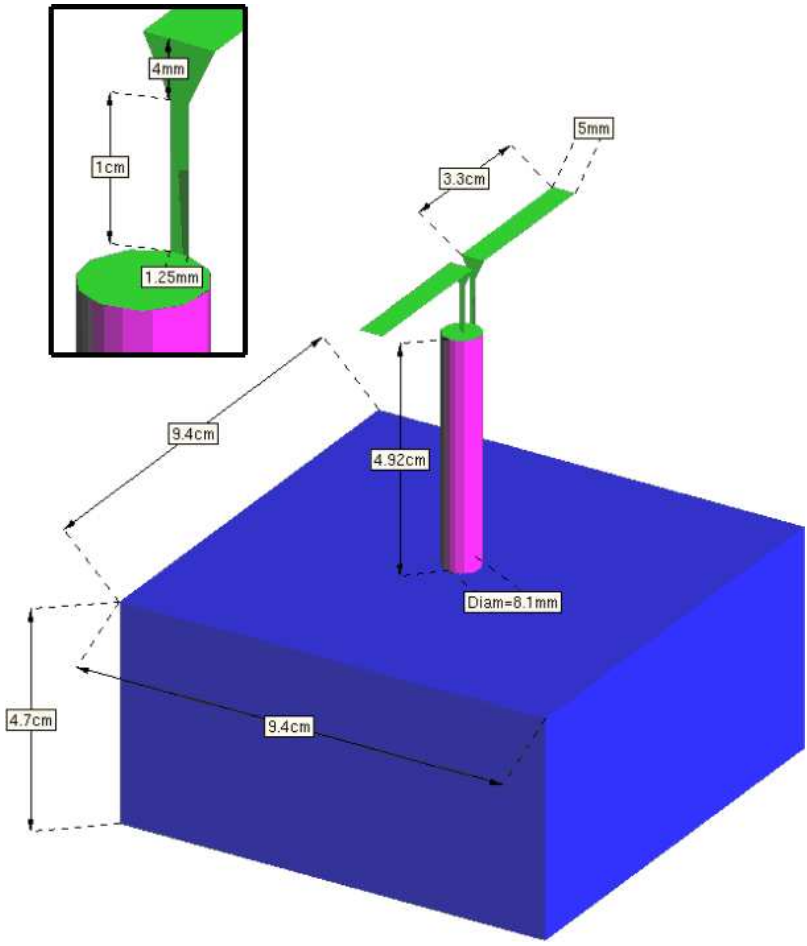

Figure 2. Dipole-on-box reference structure.

forms (Two-current Single-Equation Formulation (JM-SEqF), Dual-Equation Formulation (DEqF)); Σ_M is a sphere concentric to Σ_R, with $M_s = 2048$ sample points, so that one has a total of $M = 2048 \times 2$ measurements considering both transverse components. We note that both a fine discretization on Σ_R and strong oversampling on Σ_M with respect to the degrees of freedom in (13) has been effected in order to completely outrule possible effects of the lack of information in the results of this test. Fig. 3-top and -bottom refer to radii $R_M = 0.9\lambda$ and $R_M = 9\lambda$ respectively. For the single-current cases, the figures show both the case in which the mesh is the same as for the two-current cases,

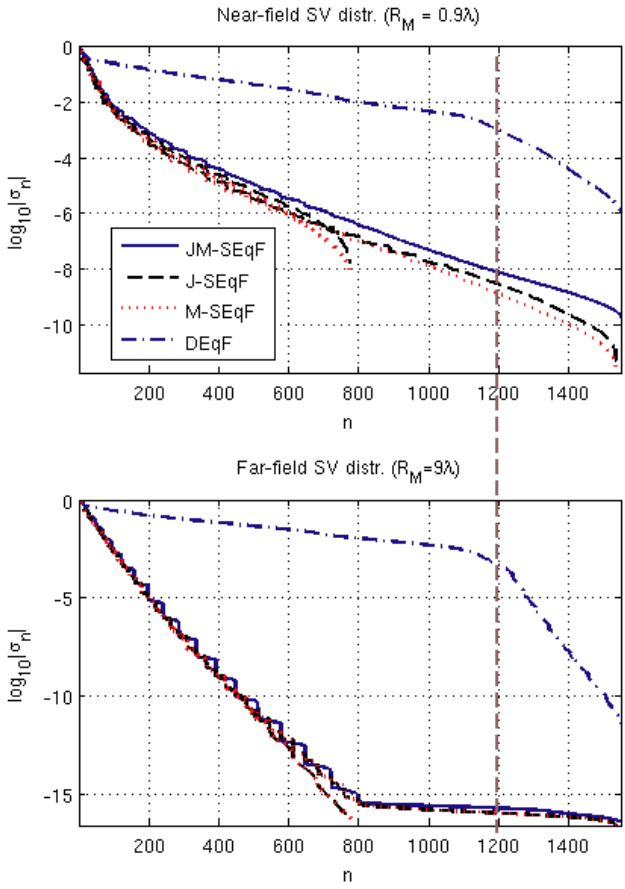

Figure 3. SV spectrum for various equivalence forms in a reconstruction problem from near- (top) and far-field (bottom) data. The shorter sequences for J-only and M-only refer to same mesh density as for J&M. Note that for the far-field case J-only and M-only sequences are identical in view of the equivalent asymptotic behavior for the associated Green's functions, while these are slightly different for the near-field case.

i.e., with half the number of unknowns, and with (approximately) the same number of unknowns as with the two currents, i.e., with a system of the same size as in Two-current Single-Equation Formulation (JM-SEqF).

We note that all Single-Equation Formulations (SEqFs) result in similar types of SV sequences, and when the number of unknowns is the same, the similarity is more pronounced; the single-current cases show a smaller condition number than the Two-current Single-Equation Formulation (JM-SEqF) case when using the same mesh as a consequence of the halved number of unknowns. It is apparent that Dual-Equation Formulation (DEqF) drastically improves the SV distribution and condition number in virtue of the availability of additional *physical* information on the solution, which, unlike conventional regularization such as low-pass filtering, does not reduce accuracy in the final solution. The similarity between the SV spectra of the Single-Equation Formulations (SEqFs), and the difference with Dual-Equation Formulation (DEqF) points at the on-surface integral equation as the key ingredient in the regularization; that was pointed out first in [5], and is similar to the treatment in [43] for a different (direct) problem.

It is important to assess the reconstruction capability expressed by the SV spectrum with respect to degrees of freedom of the measured field. With the minimum-sphere angular step indicated in (13) one arrives at 314 samples per component; considering that here we have two vector components for each of the two (independent) fields, the total number of DoF for this reconstruction problem yields $4 \times 314 = 1256$. These results hold for the "far" field (about one wavelength away from the minimum surface), but theoretical predictions [9] show that at that for both considered measurement surfaces, $R_M = 0.9\lambda$ (at a distance of about 0.5λ from Σ_R) and $R_M = 9\lambda$ the DoF are already those of the "far" field.

A remarkable result of Dual-Equation Formulation (DEqF) is the evident change in the SV slope around the spectral index 1200 (dashed vertical line in Fig. 3) that very well agrees with the DoF prediction above; within that limit, the condition number is very benign; beyond that knee point, a progressive loss of information is apparent in the increased slope, and the slope depends on the distance from the minimum sphere. No trace of the number of DoF of the measured field is apparent in the SV spectrum of Single-Equation Formulations (SEqFs). One can note that for these formulations the loss of obtainable information is dramatically worse for the far-field, while the Dual-Equation Formulation (DEqF)'s spectrum does not show such a worsening.

Finally, it is apparent that the difficulty in trying to reconstruct sources at a density beyond the one inherent to the DoF of the measured field is dramatically greater when using Single-Equation Formulations (SEqFs). Indeed, for this formulation the task is

challenging even trying to regain the number of DoF of the measured field.

3.1.2. Source Reconstruction

In this test, the reconstruction surface Σ_R is a sphere with radius $r_R = 0.5\lambda$, i.e., only slightly larger than the minimum sphere.[§] The measurement surface Σ_M is concentric with Σ_R and has radius $R_M = 8\lambda$.

A comprehensive comparison between the two two-current (Two-current Single-Equation Formulation (JM-SEqF), Dual-Equation Formulation (DEqF)) and the two single-current (J-current Single-Equation Formulation (J-SEqF), M-current Single-Equation Formulation (M-SEqF)) formulations has been performed; results are reported in Fig. 4 in a visual format, while Table 1 summarizes the quantitative indicators defined previously. Before discussing these results, it is important to discuss the meaning of the comparison, especially with respect to the reference (or "exact") solution. Our reference are the Love's currents $\mathbf{J} = \hat{\mathbf{n}} \times \mathbf{H}$ and $\mathbf{M} = -\hat{\mathbf{n}} \times \mathbf{E}$ in which the *fields* on the reconstruction surface Σ_R have been computed from the exact (MoM) current on the structure. On the other hand, the interpretation of the reconstructed currents depends on the form of the Equivalence Principle used as discussed in Section 2. Therefore, the current reconstruction error ε_R is meaningful in a strict sense only for Dual-Equation Formulation (DEqF); in all other cases, it is instead primarily a measure of the distance between Love's currents and the equivalent sources for that formulation. For example, with any of the single-current formulations one knows a priori that the reconstructed equivalent sources are not Love's, and hence one should not expect in any case ε_R to be small. Similar considerations apply for Two-current Single-Equation Formulation (JM-SEqF), but in this case it is not known a priori what the computed equivalent sources actually are; our analysis will also try to assess this from the available results.

With Two-current Single-Equation Formulation (JM-SEqF) we simply demand that the equivalent sources radiate the goal field; besides this, no relationship is enforced between electric and magnetic sources: the associated freedom is used (by the pseudo-inverse solution) to minimize the field residual and the 2-norm of the solution. Indeed, one observes that the field residual is very low as seen in Table 1, and the total current magnitude $\mathcal{M}$ is lower than with any of the

[§] The slight displacement is chosen in order to have good accuracy in the computation of reference currents from the solution; with our implementation the computation of the near field of the current radiation requires observation points to be located at a distance greater than about the cell size for each cell in the original radiator.

other forms (this is consistent with the fact that the solution of the Least-Squares (LS) normal equations leads to the minimum-energy solution [28]).

Only for Dual-Equation Formulation (DEqF) reconstructed currents resemble very well the reference, reproducing all relevant features as seen in Fig. 4. Otherwise said, Dual-Equation Formulation (DEqF) gives directly the *fields* required in diagnostic applications.

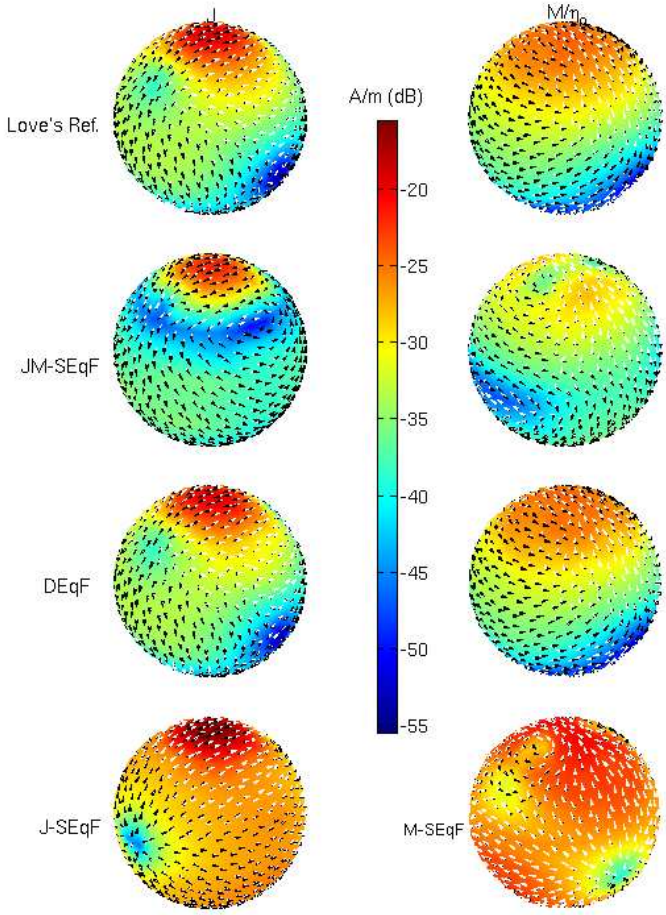

Figure 4. Reference (Love's) and reconstructed currents using various formulations for the dipole-on-box structure; test data are reported in Table 1. Black and white arrows represent direction and amplitude (relative to the total current amplitude as given by the color scale) of the real and imaginary parts of the vector currents.

Table 1. Comparison between the various equivalence formulations, dipole-on-box.

Parameter		Formulation					
		DEqF	JM-SEqF	J-SEqF		M-SEqF	
				Lo-res	Hi-res	Lo-res	Hi-res
Σ_M	$\Delta\alpha$	10°					
	N_m	1368					
	R_M	8.5λ					
Σ_R	r_R	0.5λ					
	h_R	0.1λ		0.1λ	0.07λ	0.1λ	0.07λ
	N_T	2208		1104	2280	1104	2280
$\Sigma_R^=$	N_R	7360	N/A				
	Δ	0.15λ					
Solution	ε_M	$1.3e{-}4$	$3.3e{-}7$	$9.9e{-}6$	$2.5e{-}6$	$1.3e{-}5$	$2.9e{-}6$
	ε_R	0.14	0.70	1.4	1.4	1.6	1.5
	ℓ_2 norm	0.85	0.61	1.22	1.73	1.36	1.90
	$\mathcal{P}/P_0$	0.999	$-9e-3$	0			

The single-current formulations, as expected, provide a different source distribution from Love's; we have also compared two different mesh densities: the finer mesh yields approximately the same number of unknowns as the two-currents on the other mesh. Note that amplitudes are significantly higher in this case than in the two-current approaches; for these latter, both Dual-Equation Formulation (DEqF) and Two-current Single-Equation Formulation (JM-SEqF) yield sources of the same order of magnitude. As alluded above, this should not be taken as a performance indicator in any case; in fact, we are comparing *different* quantities. The higher amplitude of the single-current case is likely to be due to the need for this single current (e.g., J) to radiate the same power as two currents jointly.

The above characteristics are reflected in the value of the reconstruction error in Table 1; again, the large values of ε_R for Single-Equation Formulations (SEqFs) do not mean that the reconstruction process is faulty: they simply indicate that the reconstructed sources are not the fields on the reconstruction surface.

As a further illustration of the actual physical meaning of the reconstructed currents, we have computed the following integral:

$$\mathcal{P} = \frac{1}{2} \iint_{\Sigma_R} \mathrm{Re}(\mathbf{J}_R^* \times \mathbf{M}_R) \cdot \hat{\mathbf{n}} ds \tag{16}$$

When reconstructed currents satisfy Love's equivalence (4) (Dual-

Equation Formulation (DEqF)), $\mathcal{P}$ in (16) is simply the total power flowing across Σ_R. For Two-current Single-Equation Formulation (JM-SEqF) it is difficult to tell since the currents are not related to actual fields in a simple way, while it is evidently zero for J-current Single-Equation Formulation (J-SEqF) and M-current Single-Equation Formulation (M-SEqF). The real part of the quantity $\mathcal{P}$ is reported at the bottom in Table 1 normalized to the actual radiated power $P_0 = |V|^2 \mathrm{Re}\,(Y)\,/2$ (power delivered to the lossless antenna port in our full-wave simulation); for Dual-Equation Formulation (DEqF) the energetic matching is very good, while Two-current Single-Equation Formulation (JM-SEqF) presents a negative $\mathcal{P}$, further illustrating the important differences between the very nature of the these equivalent currents.

A final observation is necessary to put the numeric values of reconstruction accuracy in proper perspective, also for Dual-Equation Formulation (DEqF). In this case one reconstructs Love's currents, and the comparison with reference Love's current is meaningful; however, a perfect match *cannot* be expected because of the unrecoverable loss of information on reactive fields when the measurement surface is displaced — as in real life — from the reconstruction sphere. The accuracy achieved (17% deviation) in Table 1 may not appear entirely satisfactory, but that loss of information is intrinsic: this can be verified looking at the significantly better accuracy obtained in the example in Section 3.2.

3.2. Mono-cone Antenna on a Circular Ground Plane

The structure considered is depicted in Fig. 5 along with the reconstruction surface Σ_R. It consists of a mono-cone antenna at

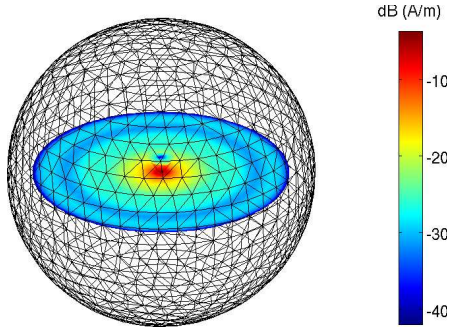

Figure 5. Mono-cone reference structure on a circular ground plane with radius 3λ showing full-wave currents for computation of reference field data and discretization of the reconstruction surface Σ_R.

Table 2. Summary of results for the mono-cone structure.

Parameter		Formulation	
		JM-SEqF	DEqF
Σ_M	$\Delta\alpha$	7.5°	
	N_m	2212	
	R_M	16.5λ	
Σ_R	h_R	0.25λ	
	r_R	2.0λ	
	N_T	5400	
Σ_R^-	N'	3276×2	N/A
	Δ	0.5λ	
Solution	ε_M	$1.95e-6$	$7.24e-5$
	ε_R	0.71	0.08
	ℓ_2 norm	0.3236	0.4583

the center of a circular ground plane with radius 1.7λ; this structure is rotationally symmetric, which allows an additional test on the quality of the reconstruction, since no symmetry is enforced on the latter. According to (13), about 1600 measurements per component are required in the far field. Details on the tests performed along with a summary of the results using Two-current Single-Equation Formulation (JM-SEqF), Dual-Equation Formulation (DEqF) are given in Table 2.

The equivalent currents computed are shown in Fig. 6; as expected, those resulting from Two-current Single-Equation Formulation (JM-SEqF) do not reflect well Love's equivalent currents; in particular, it can be seen that the shadow region clearly visible in the exact currents does not appear in the reconstructed currents. This points at the scarce information for diagnostics that can be extracted from these equivalent currents, and the risks associated to the interpretation of the results under the assumption that the reconstructed currents are actually proportional to the fields. On the other hand, Dual-Equation Formulation (DEqF) reproduces well all the relevant features, matching the reference data both in visual and quantitative terms. In addition, we see a better match of the reference currents in comparison to the previous test (dipole on box) as a result of having a reconstruction surface Σ_R relatively farther from the actual radiator (less reactive-field information is present, which in all cases is progressively masked by noise as we move away from sources to reach the measurement range). It is worth noting that reconstruction of co- and cross-polar components of the goal field is very good for both formulations, as seen in Fig. 7.

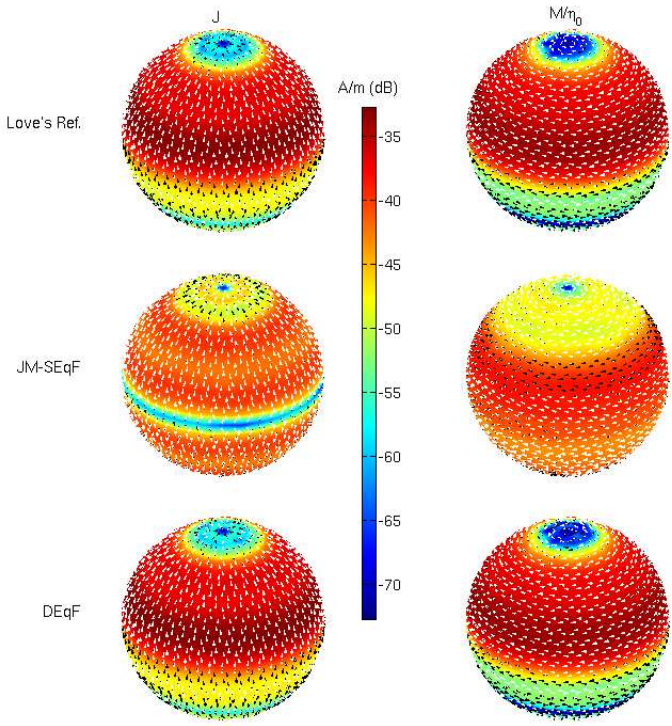

Figure 6. Reference and reconstructed equivalent currents JM-SEqF and DEqF. Black and white arrows represent direction and amplitude (relative to the total current amplitude as given by the color scale) of the real and immaginary parts of the vector currents.

4. INTERIOR AND EXTERIOR FIELDS

Given the ability shared by all formulations of reconstructing the measured fields, the distinctive aspect among those is the behavior of fields radiated inside Σ_R (in addition to the already detailed difference in the meaning of the equivalent currents). We have thus studied in more detail the field radiated by the equivalent currents in the interior region Ω_-. This will allow to check the effectiveness of the zero field enforcement for Dual-Equation Formulation (DEqF), and the nature of the solution associated to the Two-current Single-Equation Formulation (JM-SEqF); in fact, the latter has been claimed to provide Love's currents in [3, P. 3461, 27, P. 3857], which is in contrast with the theory exposed above and the numerical results, notably those in Table 1; inspection of interior fields will add visual evidence on the incorrectness of the above claims.

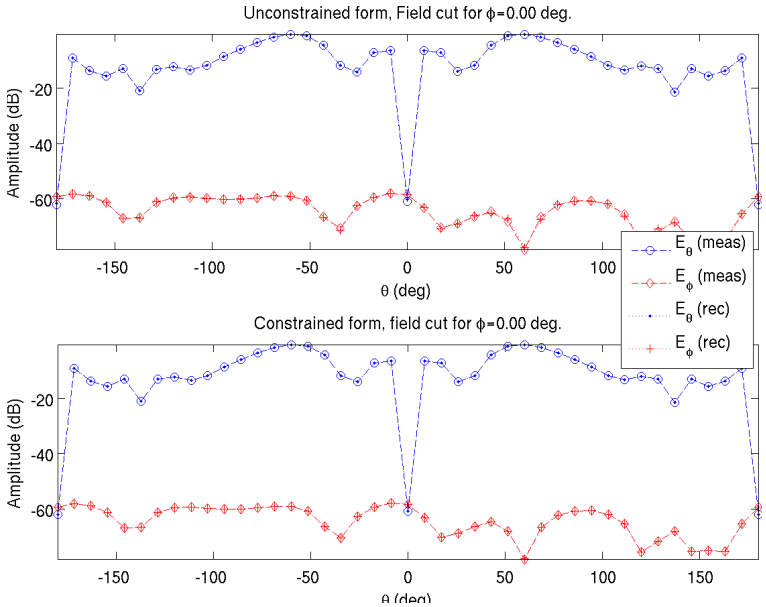

Figure 7. Reference (exact) and reconstructed field cuts for JM-SEqF (top) and DEqF (bottom).

Near fields due to currents obtained with both formulations have been computed on a vertical slice through Σ_R as seen in Figs. 8(left) and (center). The interior field for Two-current Single-Equation Formulation (JM-SEqF) is clearly *not zero*, thus ruling out once again its being related to a Love-type equivalence. As expected, Dual-Equation Formulation (DEqF) leads to negligible field inside Σ_R, while Two-current Single-Equation Formulation (JM-SEqF) generates fields that seem smooth when traversing Σ_R.

The correspondence between both formulations outside Σ_R is confirmed by the difference field, i.e., Two-current Single-Equation Formulation (JM-SEqF) minus Dual-Equation Formulation (DEqF) fields (which are in turn generated by the difference between the corresponding sources), shown in Fig. 8(right). The fact that the difference between Dual-Equation Formulation (DEqF) and Two-current Single-Equation Formulation (JM-SEqF) sources radiates non-negligible fields only inside Σ_R confirms that it results from the application of the Equivalence Principle to sources located *outside* Σ_R as discussed in Section 2.2 on the basis of the integral identities in [40]. Furthermore, it constitutes a check on the numerical implementation, since the the uniqueness theorem implies that any choice of the equivalent currents can be used in obtaining fields outside Σ_R.

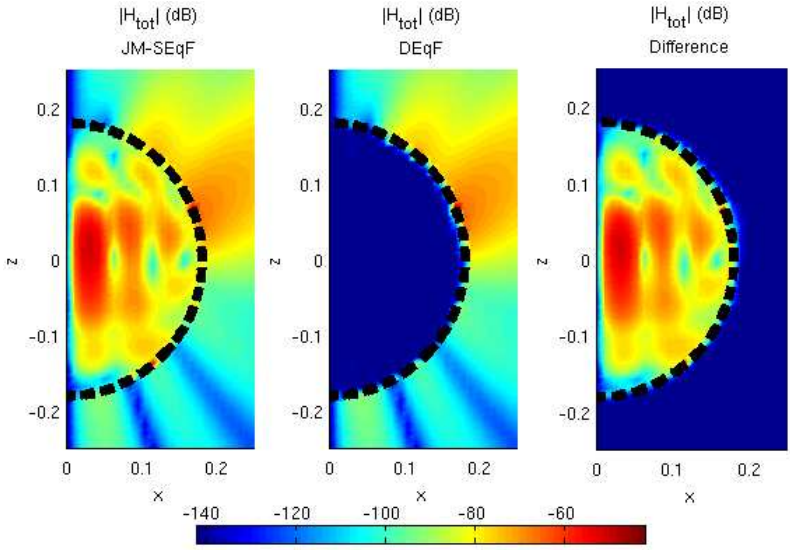

Figure 8. H-field radiated by JM-SEqF (left) and DEqF currents (right) and the difference between these (right) which is due to the element in the null-space of the radiation operator required to go from JM-SEqF into DEqF. Figure refers to a surface cutting Σ_R and the currents shown in Fig. 6).

5. TESTS WITH MEASURED DATA

In this section, we present results pertaining to measurements on a physical prototype of the structure introduced in Section 3.2. A photograph of the prototype along with the acquisition system is shown in Fig. 9. As an initial check, fields from full wave simulation (see Fig. 7) are compared to those actually measured, obtaining a good agreement in the co-polar component as seen in Fig. 10. The cross-polar component is below the noise floor (Signal to Noise Ratio (SNR) is approximately 40 dB) but has been used anyway in the reconstruction, which provides a stringent test for the technique with real data. Moreover, due to the support structure, measured data is restricted to observation coordinates for which $\theta \leq 164°$, which implies a further (typical in practice) loss of information and worsening of the Signal to Noise Ratio (SNR).

Currents were reconstructed with both Dual-Equation Formulation (DEqF) and Two-current Single-Equation Formulation (JM-SEqF); a summary of the main parameters and results is shown in

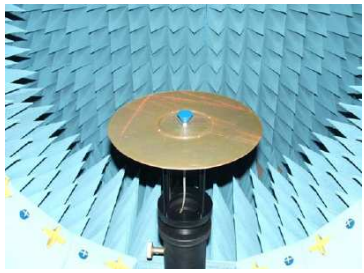

Figure 9. Prototype of mono-cone structure and the measurement range.

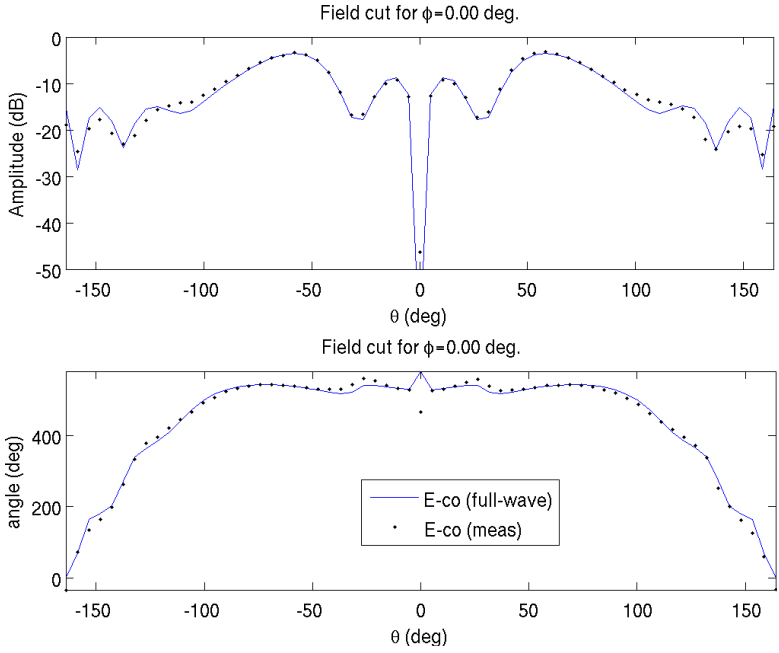

Figure 10. Comparison between measured and synthetic co-polar field for the mono-cone structure.

Table 3, while reconstructed currents are shown in Fig. 11. Even though a low data misfit ε_M is observed for both formulations (it is compatible with the Signal to Noise Ratio (SNR)), only Dual-Equation Formulation (DEqF) provides a stable solution, which agrees with the discussion in Section 3.1.1. In fact, currents from Two-current Single-Equation Formulation (JM-SEqF) are noisy, departing considerably

Table 3. Summary of results for reconstruction from measured data, mono-cone structure.

Parameter		Formulation	
		JM-SEqF	DEqF
Σ_M	$\Delta\alpha$	5.3°	
	N_m	4352	
	R_M	16.5λ	
Σ_R	h_R	0.25λ	
	r_R	2.0λ	
	N_T	5400	
Σ_R^-	N_R	N/A	900×2
	Δ		0.5λ
Solution	ε_M	$2.60e-2$	$2.80e-2$
	ε_R^*	0.90	0.20
	ℓ_2 norm	0.404	0.454

*Relative to simulation

from the ones obtained from synthetic data in Section 3.2 (the noise in the solution is especially evident in the current directions indicated by arrows). The poor spectral properties of the single-equation formulation are the cause of the solution instability mentioned above, and the necessary remedy would be regularization. This is a standard topic in inverse problems, and will be discussed here only briefly. The most employed regularizations are Tikhonov and the Truncated Singular Value Decomposition (TSVD) (e.g., [7]), but only the former is applicable in (even moderately) large problems. All regularizations imply a low-pass effect that reduces spatial resolution (much like noisy signal filtering), but especially the necessity to find the appropriate value of the regularization parameter (like the cut-off frequency of a low-pass filter) appears a major threat to generality and "blind" applicability.

In contrast, Dual-Equation Formulation (DEqF) affords a stable solution, thanks to the intrinsic regularization due to the addition of a *physical* information. Furthermore, the deviation with respect to the reference full-wave currents ε_R is very good considering the composite effect of noise and truncation, and the uncertainty due to comparing sources reconstructed from measured data to reference sources deriving from simulation. This indicates that, besides providing currents more useful in diagnostics tasks, Dual-Equation Formulation (DEqF) is more robust to noise, a key aspect when dealing with measured data.

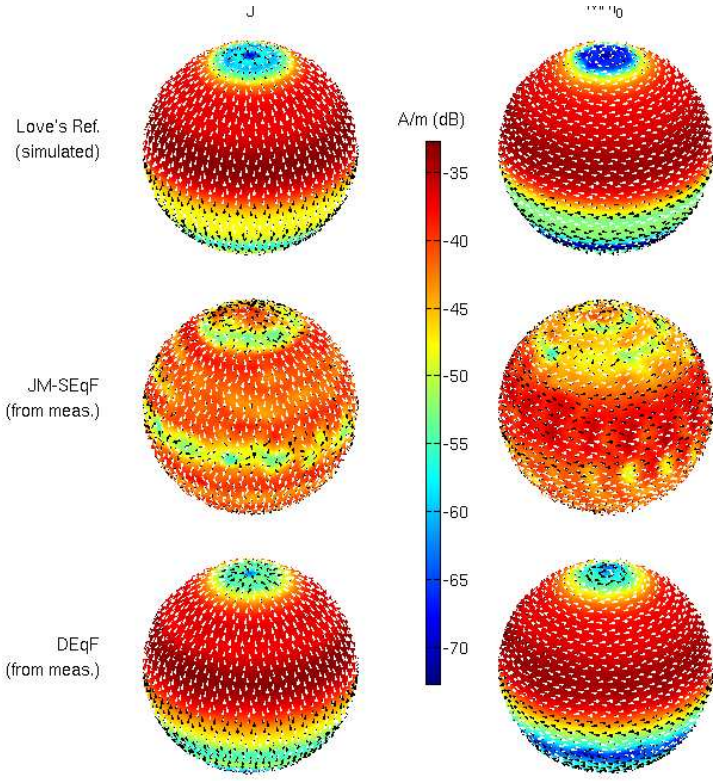

Figure 11. Equivalent currents reconstructed from measurements on the mono-cone structure; reference currents are obtained from simulation of the measured antenna. Black and white arrows represent direction and amplitude (relative to the total current amplitude as given by the color scale) of the real and imaginary parts of the vector currents.

6. CONCLUSION AND PERSPECTIVES

Various formulations of the Equivalence Principle have been analyzed in the context of the source reconstruction problem. It has been shown that if Love's equivalent sources are desired, the associated zero-field constraint needs to be enforced, resulting in a dual-equation formulation; this is opposed to the usual approaches in the literature, that employ two equivalent currents and a single integral equation.

It has been demonstrated that in its initial form, the Two-current Single-Equation Formulation (JM-SEqF) of the source reconstruction problem suffers from indeterminacy as a consequence of the existence

of a non-trivial null-space in the associated radiation operator. In practical implementation uniqueness is obtained via the implicit stipulation of a minimum-norm solution that underlies the typical pseudo-inverse solution of the discretized equations. This removes the null-space from the solution: this is shown *not* to yield Love's equivalent currents.

When solved together, the dual equations lead to correct reconstruction of Love's currents, as well as to an overall stabilization on the solution. These benefits are confirmed by tests with synthetic and measured data. As seen in the latter, the single-equation (usual) approach yields an unstable solution even for a minimal density of current unknowns, suggesting that a regularization procedure is necessary for large problems and measured data. The Dual-Equation Formulation (DEqF) solution remains stable and accurate. These benefits come to a price: a more complex operator has to be discretized, resulting in a larger matrix. However, the ability to avoid a regularization and the associated loss of resolution and difficulty in choosing the regularization parameters seems a good counterbalance to these difficulties.

This work has not addressed the computational complexity for large problems; it has however addressed the conditioning issue that is crucial for the iterative solutions necessary for large-scale computation, which is the logical step following this work.

ACKNOWLEDGMENT

The research reported herein was supported in part by the European Antenna Modeling Library initiative (EAML) of the European Space Agency (ESA); a further partial support is gratefully acknowledged for the research synergetic to the ESA Innovation Triangle Initiative (ITI).

REFERENCES

1. Alvarez, Y., F. Las-Heras, and M. R. Pino, "Reconstruction of equivalent currents distribution over arbitrary three-dimensional surfaces based on integral equation algorithms," *IEEE Transactions on Antennas and Propagation*, Vol. 55, No. 12, 3460–3468, Dec. 2007.
2. Alvarez, Y., F. Las-Heras, M. R. Pino, and J. A. Lopez, "Acceleration of the sources reconstruction method via the fast multipole method," *IEEE Antennas and Propagation Society International Symposium, 2008. AP-S 2008.*, 1–4, Jul. 2008.

3. Alvarez, Y., T. Sarkar, and F. Las-Heras, "Improvement of the sources reconstruction techniques: Analysis of the svd algorithm and the rwg basis functions," *IEEE Antennas and Propagation Society International Symposium*, 5644–5647, Jun. 2007.
4. Araque, J. and G. Vecchi, "Removal of unwanted structural interactions from antenna measurements," *IEEE Antennas and Propagation Society International Symposium, 2009. APSURSI'09.*, 1–4, Jun. 2009.
5. Araque, J. L. A. and G. Vecchi, "Improved-accuracy source reconstruction on arbitrary 3-D surfaces," *IEEE Antennas and Wireless Propagation Letters*, Vol. 8, 1046–1049, 2009.
6. Balanis, C. A., *Antenna Theory: Analysis and Design*, 3 edition, Wiley-Interscience, Apr. 2005.
7. Bertero, M. and P. Boccacci, *Introduction to Inverse Problems in Imaging*, Institute of Physics Publising, 1998.
8. Blanch, S., R. G. Yaccarino, J. Romeu, and Y. Rahmat-Samii, "Near-field to far-field transformation of bi-polar measurements by equivalent magnetic current approach," *IEEE Antennas and Propagation Society International Symposium*, 561–564, Baltimore MD, Jun. 1996.
9. Bucci, O. M., L. Crocco, and T. Isernia, "Improving the reconstruction capabilities in inverse scattering problems by exploitation of close-proximity setups," *J. Opt. Soc. Am. A*, Vol. 16, No. 7, 1788–1798, 1999.
10. Bucci, O. M. and G. Franceschetti, "On the spatial bandwidth of scattered fields," *IEEE Transactions on Antennas and Propagation*, Vol. 35, No. 12, 1445–1455, Dec. 1987.
11. Bucci, O. M. and G. Franceschetti, "On the degrees of freedom of scattered fields," *IEEE Transactions on Antennas and Propagation*, Vol. 37, No. 7, 918–926, Jul. 1989.
12. Bucci, O. M., C. Gennarelli, and C. Savarese, "Representation of electromagnetic fields over arbitrary surfaces by a finite and nonredundant number of samples," *IEEE Transactions on Antennas and Propagation*, Vol. 46, No. 3, 351–359, Mar. 1998.
13. Chew, W. C., Y. M. Wang, G. Otto, D. Lesselier, and J. C. Bolomey, "On the inverse source method of solving inverse scattering problems," *Inverse Problems*, Vol. 10, No. 3, 547–553, 1994.
14. Eibert, T. F. and C. H. Schmidt, "Multilevel fast multipole accelerated inverse equivalent current method employing Rao-Wilton-Glisson discretization of electric and magnetic surface

currents," *IEEE Transactions on Antennas and Propagation*, Vol. 57, No. 4, 1178–1185, Apr. 2009.

15. Ergul, O. and L. Gurel, "Stabilization of integral-equation formulations for the accurate solution of scattering problems involving low-contrast dielectric objects," *IEEE Transactions on Antennas and Propagation*, Vol. 56, No. 3, 799–805, Mar. 2008.
16. Vipiana, F., A. Polemi, S. Maci, and G. Vecchi, "A mesh-adapted closed-form regular kernel for 3D singular integral equations," *IEEE Transactions on Antennas and Propagation*, Vol. 56, No. 6, 1687–1698, Jun. 2008.
17. Glisson, A., "An integral equation for electromagnetic scattering from homogeneous dielectric bodies," *IEEE Transactions on Antennas and Propagation*, Vol. 32, No. 2, 173–175, Feb. 1984.
18. Golub, G. H. and C. F. van Loan, *Matrix Computations (Johns Hopkins Studies in Mathematical Sciences)*, 3rd edition, The Johns Hopkins University Press, Oct. 1996.
19. Hansen, J. E., *Spherical Near-field Antenna Measurements*, Vol. 26, IEE Electromagnetic Waves Series, Stevenage Herts England Peter Peregrinus Ltd., 1988.
20. Harrington, R. F., *Time Harmonic Electromagnetic Fields*, IEEE Press, 2001.
21. Hsiao, G. C. and R. E. Kleinman, "Mathematical foundations for error estimation in numerical solutions of integral equations in electromagnetics," *IEEE Transactions on Antennas and Propagation*, Vol. 45, No. 3, 316–328, Mar. 1997.
22. Las-Heras, F., Y. Alvarez, M. R. Pino, and M. Alvarez, "Sources reconstruction techniques for the diagnosis and characterization of antennas of complex geometry," *Proceedings of ICONIC*, 182–187, Jun. 2007.
23. Las-Heras, F., M. R. Pino, S. Loredo, Y. Alvarez, and T. K. Sarkar, "Evaluating near-field radiation patterns of commercial antennas," *IEEE Transactions on Antennas and Propagation*, Vol. 54, No. 8, 2198–2207, Aug. 2006.
24. Laurin, J. J., J. F. Zurcher, and F. Gardiol, "Near-field diagnostics of small printed antennas using the equivalent magnetic current approach," *IEEE Transactions on Antennas and Propagation*, Vol. 49, No. 5, 814–828, May 2001.
25. Leibfritz, M. M., F. M. Landstorfer, and T. F. Eibert, "An equivalent source method to determine complex excitation levels of antenna arrays from near-field measurements," *The Second European Conference on Antennas and Propagation, 2007.*

EuCAP 2007., 1–7, Nov. 2007.

26. Alvarez Lopez, Y., C. Cappellin, F. Las-Heras, and O. Breinbjerg, "On the comparison of the spherical wave expansion-to-plane wave expansion and the sources reconstruction method for antenna diangostics," *Progress In Electromagnetics Research*, PIER 87, 245–262, 2008.
27. Lopez, Y. A., F. Las-Heras Andres, M. R. Pino, and T. K. Sarkar, "An improved super-resolution source reconstruction method," *IEEE Transactions on Instrumentation and Measurement*, Vol. 58, No. 11, 3855–3866, Nov. 2009.
28. Marengo, E. A. and R. W. Ziolkowski, "Nonradiating and minimum energy sources and their fields: Generalized source inversion theory and applications," *IEEE Transactions on Antennas and Propagation*, Vol. 48, No. 10, 1553–1562, Oct. 2000.
29. Marengo, E. A. and A. J. Devaney, "The inverse source problem of electromagnetics: Linear inversion formulation and minimum energy solution," *IEEE Transactions on Antennas and Propagation*, Vol. 47, No. 2, 410–412, Feb. 1999.
30. Marengo, E. A., A. J. Devaney, and F. K. Gruber, "Inverse source problem with reactive power constraint," *IEEE Transactions on Antennas and Propagation*, Vol. 52, No. 6, 1586–1595, Jun. 2004.
31. Martini, E., G. Carli, and S. Maci, "An equivalence theorem based on the use of electric currents radiating in free space," *IEEE Antennas and Wireless Propagation Letters*, Vol. 7, 421–424, 2008.
32. Marx, E., "Integral equation for scattering by a dielectric," *IEEE Transactions on Antennas and Propagation*, Vol. 32, No. 2, 166–172, Feb. 1984.
33. Mohajer, M., S. Safavi-Naeini, and S. K. Chaudhuri, "Surface current source reconstruction for given radiated electromagnetic fields," *IEEE Transactions on Antennas and Propagation*, Vol. 58, No. 2, 432–439, Feb. 2010.
34. Nadeau, B. and J. J. Laurin, "Extrapolations using vectorial planar near-field measurements for EMC," *IEEE Int. Symp. Electromag. Compat.*, Denver CO, 924–928, Aug. 1998.
35. Persson, K. and M. Gustaffson, "Reconstruction of equivalent currents using a near-field data transformation — With radome applications," *Progress In Electromagnetics Research*, PIER 54, 179–198, 2005.
36. Petre, P. and T. K. Sarkar, "Planar near-field to far-field transformation using an equivalent magnetic current approach," *IEEE Transactions on Antennas and Propagation*, Vol. 40, No. 11,

1348–1356, Nov. 1992.

37. Petre, P. and T. K. Sarkar, "Theoretical comparison of modal expansion and integral equation methods for near-field to far-field transformation," *Asia-Pacific Microwave Conference, 1992. APMC'92.*, Vol. 2, 713–716, Aug. 1992.
38. Sarkar, T. K. and A. Taaghol, "Near-field to near/far-field transformation for arbitrary near-field geometry, utilizing an equivalent magnetic current," *IEEE Transactions on Electromagnetic Compatibility*, Vol. 38, No. 3, 536–542, Aug. 1996.
39. Sarkar, T. K. and A. Taaghol, "Near-field to near/far-field transformation for arbitrary near-field geometry utilizing an equivalent electric current and mom,"*IEEE Transactions on Antennas and Propagation*, Vol. 47, No. 3, 566–573, Mar. 1999.
40. Stratton, J. A. and L. J. Chu, "Diffraction theory of electromagnetic waves," *Phys. Rev.*, Vol. 56, No. 1, 99–107, Jul. 1939.
41. Van Den Berg, P. M., E. Korkmaz, and A. Abubakar, "A constrained conjugate gradient method for solving the magnetic field boundary integral equation," *IEEE Transactions on Antennas and Propagation*, Vol. 51, No. 6, 1168–1176, Jun. 2003.
42. Woodworth, M. B. and A. D. Yaghjian, "Derivation, application, and conjugate gradient solution of dual-surface integral equations for three-dimensional, multi-wavelength perfect conductors," *Progress In Electromagnetics Research*, PIER 5, 103–129, 1991.
43. Yla-Oijala, P. and M. Taskinen, "Well-conditioned muller formulation for electromagnetic scattering by dielectric objects," *IEEE Transactions on Antennas and Propagation*, Vol. 53, No. 10, 3316–3323, Oct. 2005.